

Self-protective Antibacterial and Hydrophobic ZnO Thin Film Coatings

M Narasimha Murthy*, M Gopi Krishna & G Chandrakala

Department of Physics, Vaagdevi Degree and PG College, Hanamkonda, Telangana 506 001 India

Received 9 October 2024; accepted 17 December 2024

The Sol-Gel dip-coating technique was used to fabricate nanostructured ZnO thin-film coatings on amorphous glass substrates. To assess the impact of annealing temperature, the coated substrates were annealed at 400, 450, and 500 °C substrate temperatures respectively. X-ray diffraction, scanning electron microscopy, and optical double-beam spectroscopy were used to evaluate the effect of annealing temperature on the structural, morphological, and optical properties of the produced thin films. The disc diffusion technique and contact angle measurements were used to examine the obtained films' hydrophobic characteristics and antibacterial activity. The obtained diffraction data revealed that all films have the polycrystalline hexagonal wurtzite crystal structure. When the annealing temperature was raised, it was observed that crystal grain sizes increased from 22.69 nm to 29 nm, indicating an improvement in crystallinity. The electronic micrographs clearly showed that the nanograins were evenly spaced over the film surface. Additionally, it was observed that increasing the annealing temperature resulted in a blue shift in the optical bandgap from 3.19eV to 3.09eV. The fabricated films showed increased antibacterial activity and hydrophobicity.

Keywords: Thin films, ZnO, Annealing temperature, Contact angle, E. coli

1 Introduction

The widespread spread of infectious diseases, such as COVID-19, due to the non-hygienic contaminated areas has become extremely popular in recent years. Physical contact with contaminated surfaces may readily transmit a variety of infections caused by microorganisms, such as bacteria, viruses, and fungi. Despite the relatively low probability of hazardous microorganisms spreading via such surfaces, several crucial conditions can significantly affect how these harmful microbes spread. Some of the elements that influence microbial adhesion to contaminated surfaces include moisture, surface roughness, and the exposure time duration that microorganisms remain stuck to a surface^{1,2}. Therefore, it is now essential to consider antimicrobial coatings that can effectively cure the spread of hazardous microbes. In addition to having antibacterial properties, nano-thin film coatings can effectively inhibit microorganisms through photo degradation³. Another option for reducing bacterial contamination from water on glass or ceramic surfaces is to apply hydrophobic nano-thin film coatings. The hydrophobic property of these nano-thin film coatings when applied to glass or ceramic surfaces is to repel the water droplets formed on solid surfaces. These coatings are frequently applied to

surgical equipment, floor tiles, and windscreens to repel contaminated water droplets. In addition, these hydrophobic thin film coatings can improve the performance as well as the lifetime of the coated surface. The treatment of microbially polluted water on solid surfaces is significantly enhanced by improving the hydrophobic and antibacterial properties of thin films. As a result, thin films with these properties provide dual benefits in ensuring hygiene and safe water quality in contaminated environments. Several metal oxide nanocoatings have been recommended for the treatment of microbial-infected surfaces. Among all of the available metal oxides, zinc oxide (ZnO) is one. ZnO has gained popularity as a potential antimicrobial coating because of its unique qualities, such as non-toxicity, thermal stability, photocatalytic capacity, antioxidant activity, and antibacterial capabilities⁴. Widyastuti *et al.*, have reported that ZnO thin film coatings fabricated by the magnetron sputtering process may be used as photocatalytic bacterial disinfection coatings⁵. Zeid *et al.*, submitted an article on the antibacterial characteristics of zinc oxide (ZnO) thin films with a nanowire surface morphology. This study reported that a variety of bacterial strains, including Escherichia coli (E. coli), have been significantly inhibited by the synthesized ZnO thin films⁶. According to Dadi *et al.*, ZnO thin films fabricated by

*Corresponding author: (E-mail: moramurthy@gmail.com)

sol-gel synthesis were very successful in drastically lowering the initial bacterial growth of *S. aureus* and *E. coli* microorganisms. This suggests that these ZnO thin film coatings are quite successful in combating harmful microorganisms⁷. Rabeel *et al.*, fabricated hydrophobic zinc oxide (ZnO) thin films and concluded that the films had a great deal of promise for application as self-cleaning coatings⁸. Shaban *et al.*, reported that the ZnO nanostructured films, which are hydrophobic even at room temperature can exhibit a wide range of advanced potential applications such as self-cleaning surface and gas-sensing coatings⁹. El-Hossary *et al.* recently submitted an article indicating that hydrophobic ZnO thin films may be used as self-cleaning, water-repellent coatings¹⁰. In this presented work, a low-cost Sol-Gel dip coating technique was used to synthesize ZnO thin films. This study's main goal is to examine how the annealing temperature impacts the characteristics of the obtained thin films and how it affects film contact angle and *E. coli* anti-bactericidal effectiveness. The results of the evaluations of contact angle and antibacterial efficacy show that the ZnO thin film coatings are best suited for antimicrobial protective applications, especially when coated on the surfaces of surgical instruments and household utensils.

2 Materials and Methodology

Methanol and zinc acetate dihydrate, both procured from SRL Chemicals in Hyderabad, India, were utilized in this process to fabricate ZnO thin films. With the aid of the TESCAN-Mira 3 electronic microscope, and the Rigaku-Smartlab XRD diffractometer, structural and surface morphology were examined. PerkinElmer-Lambda 365 spectrophotometer was used to assess the optical characteristics. The contact angle between droplets and coated thin films was determined using the Kyowa-DM501 contact angle meter.

2.1 Thin film fabrication

A homogeneous zinc solution must be prepared before starting the thin film coating process. For this purpose, 4 grams of zinc acetate dihydrate was dissolved in 100 mL of deionized water. The solution was then agitated for one hour at 60 °C using a hot plate magnetic stirrer. To achieve a gel network in the solution, it was kept in darkness for 24 hours. To fabricate ZnO thin films, the pre-cleaned glass slide is immersed vertically into the prepared zinc solution for two minutes and extracted at a regulated speed of 2 cm/mm. Each sample is dipped five times to ensure

proper adhesion in the coating process. In the last phase, the coatings were heated for an hour at 400, 450 and 500 °C in a muffle furnace and labeled Z1, Z2, and Z3, respectively.

2.2 Disc diffusion method

As part of the investigation, the disc diffusion technique was used to measure antibacterial activity. Initially, a nutrient agar medium was prepared and put onto a petri dish, where it solidified to provide a stable growth surface for the bacteria. Using sterilized swabs, the *Escherichia coli* bacterium culture was uniformly dispersed throughout the surface of the agar, ensuring equal dispersion. After the 24-hour incubation period, the produced thin films were carefully put on the agar surface such that they remained in direct contact with the bacteria. The minimum inhibitory concentration (MIC) scale was used to assess the antibacterial efficacy of thin films.

2.3 Contact angle measurements

To determine the contact angle of a liquid droplet placed on the thin film surface, the sessile drop technique was used. For this purpose, a water droplet was placed onto the ZnO-coated film substrate surface. A light source illuminates the droplet, which is then photographed by a high-resolution camera. To determine the contact angle, a tangent is drawn at the three-phase intersecting point where the liquid interface meets the solid surface.

3 Results and discussion

3.1 Crystal structure phase identification and structural analysis

The crystalline or amorphous nature of the prepared ZnO thin films can be ascertained by analyzing their X-ray diffraction spectra. The diffraction pattern of ZnO thin films fabricated is displayed in Fig. 1. The samples' diffraction peaks were indexed with the crystallographic standard database [JCPDF 36-1451]. Based on the analysis of the acquired diffraction data, it has been established that the fabricated ZnO thin films have a wurtzite hexagonal crystal structure. The diffraction patterns of each sample show that the material has multiple different distinctive peaks, indicating that it is polycrystalline. The crystal grain size (S) along the intense peak (101) is calculated using the Debye-Scherrer relation $S = k\lambda / (D \cos\theta)$ nm, where λ = X-ray wavelength (1.5405 Å), D = diffraction peak width, and 2θ = Bragg's peak position¹¹.

The unit cell volume, dislocation density, and lattice microstrain were precisely estimated using the following relationships^{12,13}.

$$\text{Unit cell volume } V = 0.866a^2c \text{ \AA}^3 \quad \dots (1)$$

$$\text{Dislocation density } \delta = \frac{1}{S^2} \text{ lines m}^{-2} \quad \dots (2)$$

$$\text{Lattice microstrain } \varepsilon = \frac{4}{B \tan \theta} \text{ lines}^{-2}/\text{m}^{-4} \quad \dots (3)$$

Based on the evaluated structural information, the following observations were noticed.

a) An increase in the size of the crystallite grains was seen as the annealing temperature was raised, indicating an improvement in the quality of the

crystal. The observed enhancement in crystal quality is consistent with the observed decrease in dislocation density and lattice strain.

b) Notably, the full width at half maximum (FWHM) of the diffraction peak corresponding to the (101) crystallographic plane, was noticed to decrease when the annealing temperature was raised. This suggests that the thin films fabricated at higher annealing temperatures might have a superior crystalline quality due to a decrease in lattice imperfections which are caused by more order of atoms on the substrate surface.

c) The crystal structure's lattice parameter ratio c/a may be used to conduct a thorough investigation of the hexagonal crystalline quality of zinc oxide (ZnO). It is feasible to conclude that the wurtzite hexagonal crystal structure of ZnO is significantly enhanced at elevated annealing temperatures as a result of the increased values of c/a ratios found in this work.

The results of the structural analysis are summarized in Table 1.

3.2 Surface morphology analysis using SEM images

Figure 2 shows electronic micrographs of thin films synthesized using Sol-Gel dip coating synthesis techniques. It has been observed that the nanosized grains are evenly dispersed across the whole surface of each thin film. In our study, the significant increase in grain size with the increase of the substrate annealing temperature from 400 to 500 °C was noticed i.e. the higher annealing temperatures result in the larger grain size formation. At higher annealing temperatures, the atoms will be supplied with enough thermal energy, which naturally enhances atom diffusion across grain boundaries which facilitates the fusing of crystal grains, resulting in the formation

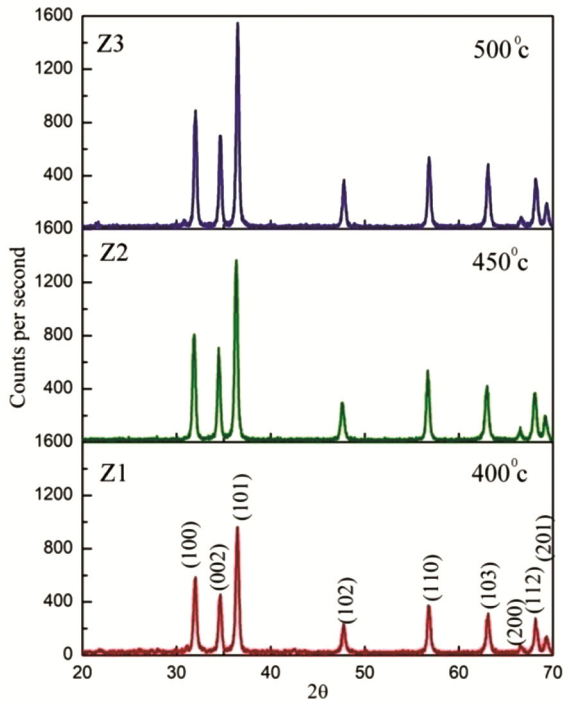


Fig. 1 — Diffraction pattern of obtained ZnO thin films deposited at various substrate temperatures

Table 1 — Structural parameters of ZnO films synthesized at different substrate temperatures

Sample	2θ	$d(\text{\AA})$	FWHM	S (nm)	$\delta (\times 10^{15})$	$\varepsilon (\times 10^{-3})$	Lattice parameters
Z-1 (400°C)	36.44	2.4637	0.3848	22.69	1.9406	5.1	$a=3.2498 \text{ \AA}$ $c=5.2033 \text{ \AA}$ $c/a=1.6011$ $V=47.59 \text{ \AA}^3$
Z-2 (450°C)	36.31	2.4726	0.3724	23.44	1.8169	4.96	$a=3.2454 \text{ \AA}$ $c=5.2058 \text{ \AA}$ $c/a=1.6040$ $V=47.48 \text{ \AA}^3$
Z-3 (500°C)	36.46	2.4621	0.3011	29.00	0.7589	3.99	$a=3.2431 \text{ \AA}$ $c=5.2087 \text{ \AA}$ $c/a=1.6061$ $V=47.44 \text{ \AA}^3$

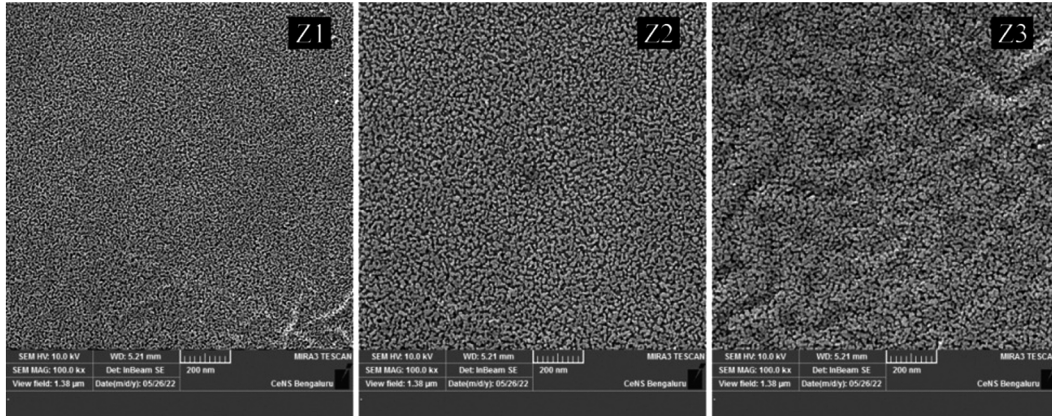


Fig. 2 — Electronic microscopic images of prepared ZnO thin films deposited at different substrate temperatures

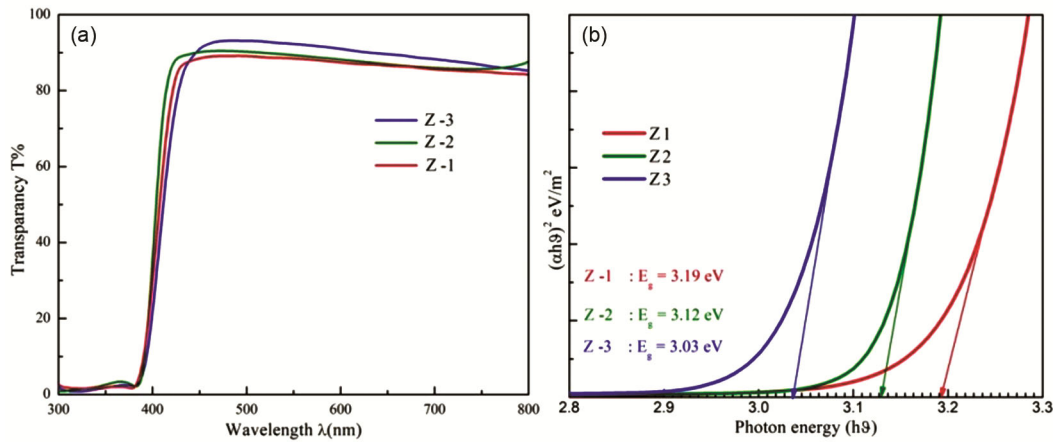


Fig. 3 — UV-Vis Spectra of ZnO thin films deposited at different substrate temperatures a) Transmission spectrum b) Tauc's plot for optical bandgap

of bigger crystalline grains. Additionally, another element that may affect grain size is the strain that develops during the film deposition process. As obtained from the diffraction data listed in Table 1, the reduced microstrain at higher substrate annealing temperatures increased grain size i.e. lattice strain relaxation could promote the grain size. There have also been prior reports of a similar tendency in which grain size increases as substrate annealing temperature increases¹⁵.

3.3 Optical properties

The optical transmittance spectrum of thin films may be used to understand thin film interactions with light at various wavelengths. These spectra can reveal some optical parameters of the film, such as its band gap, refractive index, and vital information about its composition and thickness. Fig. 3(a) demonstrates the optical transparency of the thin films in the visible region, whereas Fig. 3(b) depicts the Tauc plot used to

analyze the optical band gap. In the visible region of the transmitted spectrum, all the fabricated ZnO thin films had transparency higher than 81%. Film annealed at 500 °C has better optical transparency than films annealed at lower temperatures i.e. 400 and 450 °C. This increase in transparency can be explained by the smoother surface caused by a decrease in surface roughness at higher annealing temperatures. A smoother film surface reduces light scattering, allowing more light to penetrate through the film¹⁶. According to the diffraction data summarized in Table 1, increasing annealing temperature has promoted an increase in grain size and a decrease in dislocation density, resulting in fewer grain boundaries and surface active sites, which are the principal contributors to light scattering¹⁷. As a result of these structural changes, the fabricated thin films' optical transparency in the visible region was found enhanced. The optical bandgaps obtained for films Z-1, Z-2, and Z-3 are 3.19 eV, 3.12 eV, and

3.03 eV, respectively. One possible explanation for the decrease in optical bandgap as annealing temperature rises can be the increment of crystal grain size¹⁸. The previously published reports indicated that higher annealing temperatures lead to an increase in the crystal grain size, showing an enhancement in the crystalline quality of the ZnO phase¹⁹. It has previously been shown that when films are baked at different annealing temperatures, the enhanced crystalline quality results in a decrease in optical bandgap²⁰. The refractive index (n) of fabricated ZnO thin films can be calculated using the optical bandgap based on the following relation²¹. A detailed description of the acquired optical parameters is included in Table 2.

$$1 - \sqrt{\frac{E_g}{20}} = \frac{n^2 - 1}{n^2 + 1} \quad \dots (4)$$

3.4 Thin film surface Contact angle measurements

The contact angle of a 4μL water droplet with the synthesized ZnO thin films was measured using the sessile drop method. The evaluation of contact angles was carried out in two distinct modes: before and after exposure to external UV light. Fig. 4 gives a detailed illustration of the contact angles of water droplets made with the fabricated ZnO thin films. The contact angle values obtained for samples Z1, Z2, and Z3 are 96.02°, 104.33°, and 108.66°, respectively,

Table 2 — Optical parameters of ZnO thin films deposited at different substrate temperatures

Sample	Transmission (T%)	Bandgap E _g (eV)	Refractive index (n)
Z1	81	3.19	2.3477
Z2	82	3.12	2.3654
Z3	84	3.03	2.3890

but in the presence of UV light exposure, these values decreased to 94.32°, 102.02°, and 103.41°, respectively. It is evident that the corresponding contact angles in both situations rise with annealing temperature but are found to decrease when droplets are exposed to UV light.

However, it should be noted that in both these cases, the films maintain their hydrophobicity. The following assumption may be used to explain why thin films that have been exposed to UV light exhibit a reduction in contact angles: Electron-hole pairs are created when a drop of water on a thin film surface is exposed to UV radiation. These pairs can interact with the oxygen atom that the ZnO lattice has released. Thus, in the ZnO lattice, oxygen vacancies can be formed which then may adsorb -OH functional groups from water droplets which may directly decrease the contact angle²². Furthermore, when the annealing temperature increases, the decreased surface roughness and improved film adhesion to the substrate might also contribute to the hydrophobic character of the films^{23,24}.

3.5 Antibacterial activity

Figure 5 depicts the antibacterial activity of ZnO thin films fabricated at various annealing

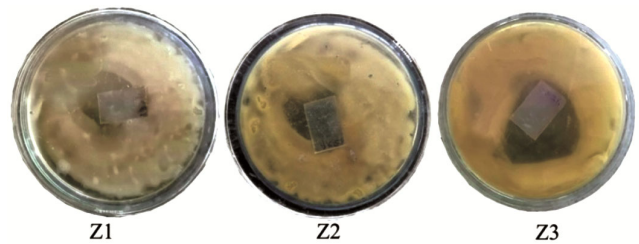


Fig. 5 — Antibacterial ability of ZnO thin films deposited at different substrate temperatures against E. Coli microorganism

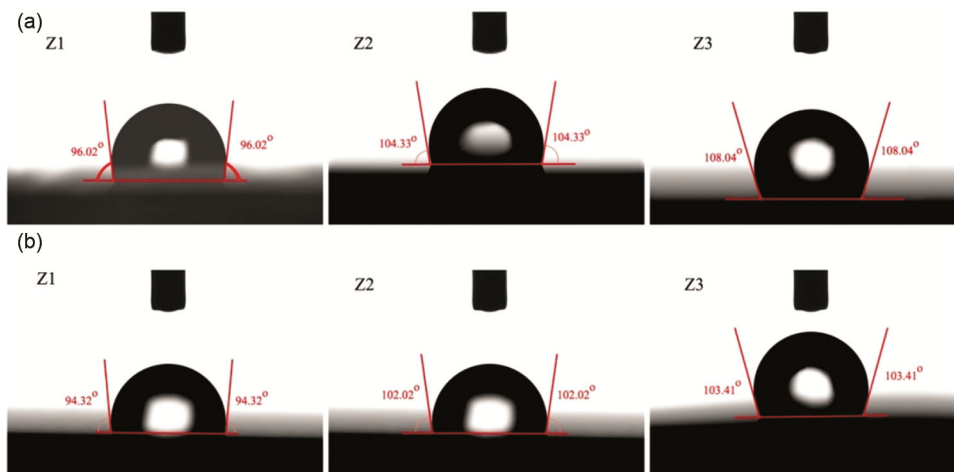


Fig. 4 — Contact angles of ZnO thin films deposited at different substrate temperatures a) Exposed to normal light b) Exposed to UV light.

temperatures against the bacterium *E. Coli*. Generally, the degree of inhibition is used to evaluate the antibacterial effectiveness of thin films. The inhibitory zones measured in this study at temperatures 400, 450 and 500 °C were 13 mm, 17 mm, and 21 mm, respectively. i.e. it may be convenient that the antibacterial effectiveness of the obtained ZnO thin films rises with increasing annealing temperature.

It is thought that surface alterations, such as changes in surface texture and crystallography significantly affect how easily bacteria adhere to surfaces. The antibacterial efficiency of fabricated ZnO thin films against *Escherichia coli* may be explained by considering crystal grain size. The crystal grain size, which grows directly proportional to annealing temperature results in the enhancement of bacterial adherence to the film's surface. Hence the increase in grain size significantly improves bacteria's ability to stick to the film surface leading to an effective bacterial inhibition. Nanoparticles have a substantially larger surface area due to their tiny size as compared to the bulk form of materials. This increase in surface area subsequently causes the number of active sites on the surface of the particles to rise. An increase in active sites greatly enhances the nanoparticles' ability to bind harmful microorganisms for extended periods. Simultaneously, the nanoparticles promote the formation of electron and hole pairs when exposed to light. When these pairs come into contact with the atmospheric water molecules, superoxide ions, and hydroxyl radicals are produced²⁵. These reactive agents are called reactive oxygen species (ROS). The bacterial cell wall is severely disrupted as a result of these ROS species' interaction with the bacterial cell wall. This disruption is crucial because it has the potential to accelerate the deterioration of proteins and DNA which are necessary for harmful bacterial growth²⁶. Furthermore, the release of zinc cations (Zn^{2+}) from ZnO nanoparticles of the thin films is another mechanism by which harmful bacteria cell walls can be damaged²⁷.

4 Conclusion

Using a low-cost dip coating technique, wurtzite hexagonal crystal structured ZnO thin films were successfully synthesized at different annealing temperatures. Electronic microscopic studies revealed that the grain sizes of the ZnO thin films grow with annealing temperature, indicating enhancement of crystalline quality. Increasing annealing temperatures

to 400, 450, and 500 °C resulted in an increase in grain size from 22.69 nm to 29 nm and a drop in dislocation density from 1.9406×10^{15} to 0.7589×10^{15} lines m^{-2} . This shows that the crystalline quality of ZnO has improved with the annealing temperature. Optical studies revealed a decrease in the optical bandgap from 3.19eV to 3.09eV, owing to improved crystalline structure. The fabricated thin films' hydrophobic characteristics towards water droplets were validated by contact angle measurements. Nevertheless, the contact angles decreased when exposed to UV radiation, but the films still maintained their hydrophobic properties, indicating their water-repellent properties. The inhibition zone was measured to assess antibacterial efficiency against *E. Coli* microorganisms, and it increased from 13mm to 21mm. This suggests that the obtained films are capable of killing the bacterium. The hydrophobic characteristics and improved antibacterial activity of ZnO thin films prepared at high annealing temperatures can make them suitable for use as self-protective, water-resistant coatings.

Acknowledgments

In connection with this work, the authors would like to thank Dr. C. J Sreelatha, Professor of Physics, Kakatiya University, India, and Dr V. Ganesh, Assistant professor of Physics, King Khalid University, Saudi Arabia for their valuable suggestions during this work.

Conflict of interest

The authors explicitly declare, by this statement, that they have no conflicts of interest.

References

- 1 Stanaszek T & Elzbieta, *Coatings*, 10 (2020) 1203.
- 2 Miranda R C & Schaffner D W, *Appl. Environ. Microbiol*, 82 (2016) 6490.
- 3 Widyastuti, Endrika, Xu F Y, Chiu C T, Jan J H, Hsu J L & Lee Y C, *Catalysts*, 11 (2021) 1416.
- 4 Puspasari V, Ridhova A, Hermawan A, Amal M I & Khan M M, *Bioprocess Biosyst Eng*, 45 (2022) 1421.
- 5 Widyastuti E, Hsu J L & Lee Y C, *Nanomaterials*, 12 (2022) 463.
- 6 Zeid Abou, Souad, Anne Perez, Stéphane Bastide, Marie Le Pivert, Stéphanie Rossano, Hynd Remita, Nicolas Hautière & Yamin Leprince-Wang, *Coatings*, 14 (2023) 41.
- 7 Dadi R, Kerignard E, Traoré M, Mielcareck C, Kanaev A & Azouani R, *Chem Eng Trans*, 84 (2021) 13.
- 8 Rabeel M, Javed S, Khan R, Akram M A, Rehman S, Kim D K & Khan M F, *Materials*, 15 (2022) 3364.
- 9 Shaban M, Zayed M & Hamdy H, *RSC Adv*, 7 (2017) 617.

- 10 El-Hossary F M, Mohamed S H, Noureldein E A & Abo El-Kassem M, *Bull Mater Sci*, 44 (2021) 1.
- 11 Thiruvengadathan R, Dhua S, Rani S, Mathai C J, Bai M, Gangopadhyay K & Gangopadhyay S, *Mater Adv*, 3 (2022) 5383.
- 12 Alsaad A M, Ahmad A A, Al-Bataineh Q M, Bani-Salameh A A, Abdullah H S, Qattan I A, Albataineh Z M & Telfah A D, *Materials*, 13 (2020) 1737.
- 13 Al-Bataineh Q M, Telfah M, Ahmad A A, Alsaad A M, Qattan I A, Baaziz H & Charifi Z & Telfah A, *Photonics*, 7 (2020) 112.
- 14 Saha J K, Bukke R N, Mude N N & Jang J, *Sci Rep*, 10 (2020) 8999.
- 15 Mazur M, Kielczawa S, Domaradzki J, *Coatings*, 12 (2022) 1885.
- 16 Liu W J, Chang Y H, Chiang C C, Chen Y T, Lin C C, Liao Y C & Lin S H, *Results Opt*, 6 (2024) 100636.
- 17 Sendi R, *J Umm Al-qura Univ Appl Sci*, 8 (2022) 50.
- 18 Tsega Yihunie M, *J Nanomater*, 2023 (2023) 3098452.
- 19 Ruiz-Perona A, Sanchez Y, Guc M, Kodalle T, Placidi M, Merino J M, Cabello F, García-Pardo M & León M Caballero R, *J Phys Mater*, 4 (2021) 034009.
doi: 10.11648/j.ajm.20210701.15
- 20
- 21 Ibrahim S, Ali A A & Fathi A M, *Sci Rep*, 14 (2024) 8518.
- 22 Tański T, Zaborowska M, Jarka P & Woźniak A, *Sci Rep*, 12 (2022) 11329.
- 23 Silva H D S, Marciano F R, de Menezes A S, de Carvalho Costa T S, de Almeida L S, Rossino L S, Nascimento I O, de Sousa R R M & Viana B C, *J Mater Res Technol*, 9 (2020) 13945.
- 24 Liu W J, Chang Y H, Chiang C C, Chen Y T, Lu P X, He Y J & Lin S H, *Coatings*, 13 (2023) 1783.
- 25 He Y, Zan J, He Z, Bai X, Shuai C & Pan H, *Nanomaterials*, 14 (2024) 452.
- 26 Amaro F, Morón A, Díaz S, Martín-González A & Gutiérrez J C, *Microorganisms*, 9 (2021) 364.
- 27 Kalra K, Chhabra V & Prasad N, *J Phys.: Conf Ser*, 2267 (2022) 012049.